

## Intrasubband and intersubband plasmons in a semi-infinite Fibonacci HgTe/CdTe superlattice

Dan-hong Huang

*China Center of Advanced Science and Technology (World Laboratory), P.O. Box 8730, Beijing,  
People's Republic of China  
and Department of Physics, Fudan University, Shanghai, China*

Jian-ping Peng and Shi-xun Zhou

*Department of Physics, Fudan University, Shanghai, China  
(Received 10 April 1989)*

An equivalent-transfer-matrix theory is proposed by introducing the formal structure factors to study the intrasubband and intersubband plasmons in a semi-infinite Fibonacci HgTe/CdTe superlattice. Taking into account the hybridization between the interface states and the heavy-hole-like states, we find several new surface-plasmon branches. In such a system, the bulk- and the surface-plasmon spectra will exhibit many different features when the surface layer of the superlattice is selected at different positions. It may provide us with useful information about the selection of the surface-plasmon branch that we need for surface-wave device application.

### I. INTRODUCTION

There has been a great deal of recent theoretical interest in the properties of layered electron gas<sup>1</sup> (LEG) and one-dimensional<sup>2,3</sup> (1D) quasiperiodic systems. These systems show critical states in a way similar to electrons. Critical states exist precisely at the mobility edge. A more significant development for Fibonacci systems is the recent fabrication<sup>4</sup> by Merlin *et al.* of semiconductor Fibonacci superlattices. On the other hand, Huang and Zhou<sup>5,6</sup> have proposed the theory of collective excitations in HgTe/CdTe superlattices.

A HgTe/CdTe superlattice is an attractive material to work with, consisting of both a semimetal and a wide-band-gap semiconductor. The  $\Gamma_6$ - $\Gamma_8$  energy bands in HgTe layers are inverted relative to those in CdTe layers to give the zero band gap. The computations of the band structure of the HgTe/CdTe superlattice given by plane-wave method (PWM),<sup>7</sup> linear combination of atomic orbitals (LCAO),<sup>8,9</sup> and envelope-function approximation<sup>10,11</sup> (EFA) methods agree well and show that the electronlike, heavy-hole-like, and light-hole-like states are, as expected, confined very well in HgTe and CdTe layers.<sup>9,12,13</sup> On the other hand,  $\Gamma_8$  energy bands in both HgTe and CdTe layers possess the effective masses with opposite signs on each side of the interface, respectively, which directly leads to the formation of a quasi-interface state with its energy lying in the range  $0 < E_i < \Lambda$ , where  $\Lambda = V_p$  is the separation of  $\Gamma_8$  energy bands in both HgTe and CdTe layers. Clearly, the electrons in HgTe layers will be in the quasi-interface states localized near the interface with the energy  $E_i < \Lambda$ . Moreover, light holes in CdTe layers will also be in the anomalous quasi-interface states localized near the interface, owing to the negative effective mass of the light hole. All of these results are as a consequence of matching the bulk states belonging to the conduction band in HgTe with those belonging to the

light-hole valence band in CdTe. This match is only favorable when the bulk states to be connected are made of atomic orbitals of the same symmetry type and the effective masses on either side of the interface have opposite signs. As a collective excitation model, we can treat the interface states in HgTe and CdTe layers separately, as two different kinds of quasiparticles with the effective masses  $M_E$  and  $M_{LH}$ , just as the model given by Lin-Liu and Sham.<sup>8,10</sup>

It is proved that the thickness of materials HgTe and CdTe will mainly determine the width of the band gap and subbands, respectively. We assume that the layers of HgTe and CdTe have the same thickness  $d/2$  and that  $d$  is smaller than the critical thickness so that the superlattice will behave like a semiconductor. Besides, we consider the motion of quasiparticles in the layers to be completely free. If  $d$  is not too small, we can neglect the tunneling effects coming from the overlap of interface states localized at adjacent interfaces in the quantum well. Indeed, when the magnitude of the planar wave vector  $k_{\parallel}$  is not very small, the hybridization between the interface states and the heavy-hole-like states will affect the fundamental gap of the material, which contributes a great deal to the transport and the optical absorption.<sup>12,13</sup> The band nonparabolicity shows a small effect on the lower subband excitations within a quantum well.<sup>14</sup> We have partly taken this effect into consideration by using wave functions with a finite width of localization at interfaces, and including the coupling between the interface states and heavy-hole-like states. If we confine the study of collective excitation to the case in which the transitions of single particle are limited to the neighborhood of the  $\Gamma$  point of energy bands in the  $k$  space, we can neglect the hybridization in the band structure.<sup>5,6</sup> However, this hybridization can be taken into account by using a two-band tight-binding model.

Conspicuous by its absence in the literature, however, is a calculation of the intrasubband and intersubband

plasmons associated with the interface states in Fibonacci HgTe/CdTe superlattice and intersubband plasmons in general type-I and type-II Fibonacci superlattices. The goal of this paper is to give the calculation of plasmon excitations in the semi-infinite Fibonacci HgTe/CdTe superlattice, where a rich spectrum is expected. The paper is organized as follows. In Sec. II, the equivalent-transfer-matrix theory is presented, which can also be used to study the intersubband plasmons in general type-I and type-II Fibonacci superlattices. In Sec. III, the numerical calculations of bulk and surface intrasubband plasmons, as two examples for comparison, have been given in the periodic and quasiperiodic HgTe/CdTe superlattices, respectively. Concluding remarks and a discussion are contained in Sec. IV.

## II. THE EQUIVALENT-TRANSFER-MATRIX THEORY

Let us consider  $F_m$  minicells, shown in Fig. 1(a), where  $F_m$  is a Fibonacci number, i.e.,  $F_m$  satisfies the recursion relation  $F_{m+1} = F_m + F_{m-1}$ , for  $m \geq 1$ , with  $F_0 = 1$ , and  $F_1 = 1$ . The widths of minicell  $A$  and minicell  $B$  are chosen as  $d_A$  and  $d_B$ , respectively. In the  $m$ th generation there are  $F_m$  elements of the quasi-one-dimensional "string".<sup>1</sup> This includes  $F_{m-1}$  minicells  $A$  and  $F_{m-2}$  minicells  $B$ , e.g., the second generation corresponds to

the string  $AB$ , and the third generation corresponds to the string  $AB A$ . The ratio of the number of minicells  $A$  to the number of minicells  $B$  approaches the golden mean  $\tau = (1 + \sqrt{5})/2$ . The unit cell of the superlattice is then composed of  $F_m$  elements of the string. In contrast with the general Fibonacci model<sup>1</sup> in which the bulk-plasmon spectrum remains unchanged, although the surface-plasmon spectrum may exhibit many different features, the minicell introduced here will produce three different features of the bulk-plasmon spectra.

Considering the existence of the distribution of wave functions associated with interface states and bound heavy-hole-like states within a quantum well, we generalize the simpler transfer matrix given by Hawrylak *et al.*<sup>1</sup> referred to the ideal charged layer by introducing the formal structure factors  $S_E$ ,  $S_{LH}$ , and  $S_{HH}$  for electronlike, light-hole-like, and heavy-hole-like states, respectively. Thus the charged interface and slab within the quantum well can be equivalently regarded as an "ideal" charged layer again. Without repeating a lengthy derivation similar to that of Ref. 1, we directly write down the equivalent transfer matrices for minicell  $A$  and minicell  $B$ , respectively:

$$\underline{T}_A = \underline{T}_{LH}(d_A/4) \underline{T}_{HH}(d_A/4) \underline{T}_E(d_A/2), \quad (1)$$

$$\underline{T}_B = \underline{T}_{LH}(d_B/4) \underline{T}_{HH}(d_B/4) \underline{T}_E(d_B/2), \quad (2)$$

with  $\underline{T}_E$ ,  $\underline{T}_{LH}$ , and  $\underline{T}_{HH}$ , in turn, given by

$$\underline{T}_E(d/2) = \begin{bmatrix} [1 + S_E^{-1}(d)] \exp(-qd/2) & S_E^{-1}(d) \exp(qd/2) \\ -S_E^{-1}(d) \exp(-qd/2) & [1 - S_E^{-1}(d)] \exp(qd/2) \end{bmatrix}, \quad (3)$$

$$\underline{T}_{LH}(d/4) = \begin{bmatrix} [1 + S_{LH}^{-1}(d)] \exp(-qd/4) & S_{LH}^{-1}(d) \exp(qd/4) \\ -S_{LH}^{-1}(d) \exp(-qd/4) & [1 - S_{LH}^{-1}(d)] \exp(qd/4) \end{bmatrix}, \quad (4)$$

$$\underline{T}_{HH}(d/4) = \begin{bmatrix} [1 + S_{HH}^{-1}(d)] \exp(-qd/4) & S_{HH}^{-1}(d) \exp(qd/4) \\ -S_{HH}^{-1}(d) \exp(-qd/4) & [1 - S_{HH}^{-1}(d)] \exp(qd/4) \end{bmatrix}, \quad (5)$$

where the formal structure factors  $S_E$ ,  $S_{LH}$ , and  $S_{HH}$  are the relevant variables. The matrices  $\underline{T}_E$ ,  $\underline{T}_{LH}$ ,  $\underline{T}_{HH}$ ,  $\underline{T}_A$ , and  $\underline{T}_B$  are  $2 \times 2$  matrices with unit determinant. Note that the string of matrices  $\{\underline{T}_A (\underline{T}_B)\}$  is a Fibonacci sequence of matrices of  $\underline{T}_A$  and  $\underline{T}_B$   $\{\dots \underline{T}_A \underline{T}_B \underline{T}_A \underline{T}_B \underline{T}_A \underline{T}_B \underline{T}_A \underline{T}_B \underline{T}_A\}$ . Equations (1) and (2) are conveniently studied by the rational approximation method. A rational approximation  $m$  to a Fibonacci sequence consists of a periodic sequence of unitcells containing  $F_m$  matrices  $T_A$  and  $T_B$  corresponding to the different minicells  $A$  and  $B$  in the  $m$ th generation of the Fibonacci sequence. The bands consist of those values of the formal structure factors  $S_E$ ,  $S_{LH}$ , and  $S_{HH}$  for which the trace of the equivalent transfer matrix across the unit cell is between  $-2$  and  $+2$ . For the sake of comparison with the results given by the self-consistent-field (SCF)

theory,<sup>5,6</sup> we let  $m = 1$ , corresponding to the periodic HgTe/CdTe superlattice, and neglect the contribution of the heavy-hole-like states for the time being, then we get

$$\underline{T}_d = \underline{T}_{LH}(d/2) \underline{T}_E(d/2). \quad (6)$$

The rational approximation will give

$$1 - (S_E^{-1} + S_{LH}^{-1})S + S_E^{-1} S_{LH}^{-1} [S^2 - (S')^2] = 0, \quad (7)$$

where  $S$  and  $S'$  are the screening functions given by

$$S = \sinh(qd) / [\cosh(qd) - \cos(q_z d)], \quad (8)$$

$$S' = 2 \sinh(qd/2) \cos(q_z d/2) / [\cosh(qd) - \cos(q_z d)]. \quad (9)$$

On the other hand, the SCF theory<sup>5,6</sup> gives

$$1 - (\chi_E + \chi_{LH})[B - 2\chi_E\chi_{LH}B(A - B)/(\chi_E + \chi_{LH})]S + \chi_E\chi_{LH}[S^2 - (S')^2]B^2 - (A - B)[(\chi_E + \chi_{LH}) - \chi_E\chi_{LH}(A - B)] = 0, \quad (10)$$

where  $\chi_E$  and  $\chi_{LH}$  stand for the susceptibilities of electron and light hole, respectively, and the symbols  $A, B$  are defined as the screened Coulomb interaction,<sup>5,6</sup> which will be explicitly written out below. Comparing Eq. (7) with Eq. (10), we can easily get

$$S_E^{-1} = \chi_E B / [1 - \chi_E(A - B)], \quad (11)$$

$$S_{LH}^{-1} = \chi_{LH} B / [1 - \chi_{LH}(A - B)]. \quad (12)$$

From Eqs. (11) and (12) we easily know that

$$S_{HH}^{-1} = \chi_{HH} G / [1 - \chi_{HH}(V - G)], \quad (13)$$

where the symbols  $V$  and  $G$  are similar to  $A$  and  $B$ , and will be also explicitly written out below. It is really a quite intuitive result, i.e., if we replace  $S_{HH}$  in Eq. (13) by  $S$  in Eq. (8), then we can obtain the collective excitation spectrum in a general type-I superlattice.

For the intrasubband mode, we have<sup>5,6</sup>

$$\chi_E(q, \omega) = n_E q^2 / m_E \omega^2 (2\pi e^2 / \epsilon_s q), \quad (14a)$$

$$\chi_{LH}(q, \omega) = n_{LH} q^2 / m_{LH} \omega^2 (2\pi e^2 / \epsilon_s q), \quad (14b)$$

$$\chi_{HH}(q, \omega) = n_{HH} q^2 / m_{HH} \omega^2 (2\pi e^2 / \epsilon_s q), \quad (14c)$$

and

$$A = \{4[2 + \exp(-\beta d / 2)] / [d + 2 \sinh(\beta d / 2) / \beta]^2\} \\ \times \{2q / (q^2 - 4\beta^2) [\sinh(\beta d / 2) / \beta + \sinh(\beta d) / 4\beta + d / 4] + [d + 2 \sinh(\beta d / 2) / \beta] / q \\ - \{\exp[-(2\beta + q)d / 4] / (2\beta + q) - \exp[(2\beta - q)d / 4] / (2\beta - q) \\ + 2 \exp(-qd / 4) / q\} \{ \sinh[(2\beta + q)d / 4] / (2\beta + q) + \sinh[(2\beta - q)d / 4] / (2\beta - q) \\ + 2 \sinh(qd / 4) / q \}, \quad (15a)$$

$$B = \{4[2 + \exp(-\beta d / 2)] / [d + 2 \sinh(\beta d / 2) / \beta]^2\} \\ \times \{ \sinh[(2\beta + q)d / 4] / (2\beta + q) + \sinh[(2\beta - q)d / 4] / (2\beta - q) + 2 \sinh(qd / 4) / q \}^2, \quad (15b)$$

$$V = G = 1. \quad (15c)$$

Here we have introduced the  $\delta$ -function approximation<sup>5</sup> in Eq. (15c).

For the intersubband mode, on the other hand, we have<sup>5,6</sup>

$$\chi_E(\mathbf{q}, \omega) = 2n_E \Omega_{10} / \hbar (\omega^2 - \Omega_{10}^2) (2\pi e^2 / \epsilon_s q), \quad (16a)$$

$$\chi_{LH}(\mathbf{q}, \omega) = [2n_{LH} \Omega_{10} / \hbar (\omega^2 - \Omega_{10}^2)] (2\pi e^2 / \epsilon_s q), \quad (16b)$$

$$\chi_{HH}(\mathbf{q}, \omega) = \{2n_{HH} \Omega_{10}^* / \hbar [\omega^2 - (\Omega_{10}^*)^2]\} (2\pi e^2 / \epsilon_s q), \quad (16c)$$

and

$$A = \{8 / [4 \sinh^2(\beta d / 2) / \beta^2 - d^2]\} \{q [\sinh(\beta d) - \beta d] / [2\beta(q^2 - 4\beta^2)] \\ + \{\exp[-(2\beta + q)d / 4] / (2\beta + q) + \exp[(2\beta - q)d / 4] / (2\beta - q)\} \\ \times \{ \sinh[(2\beta + q)d / 4] / (2\beta + q) - \sinh[(2\beta - q)d / 4] / (2\beta - q) \}, \quad (17a)$$

$$B = \{-8 / [4 \sinh^2(\beta d / 2) / \beta^2 - d^2]\} \{ \sinh[(2\beta - q)d / 4] / (2\beta - q) - \sinh[(2\beta + q)d / 4] / (2\beta + q) \}^2, \quad (17b)$$

$$V = (qd / 2) \{1 / [(qd / 2)^2 + \pi^2] + 1 / [(qd / 2)^2 + 9\pi^2]\} \\ - (qd)^2 \cosh(qd / 4) \exp(-qd / 4) \{1 / [(qd / 2)^2 + \pi^2] - 1 / [(qd / 2)^2 + 9\pi^2]\}^2, \quad (17c)$$

$$G = -(qd)^2 \cosh^2(qd / 4) \{1 / [(qd / 2)^2 + \pi^2] - 1 / [(qd / 2)^2 + 9\pi^2]\}^2, \quad (17d)$$

where we have assumed  $L_{\text{HH}} = d/2$  in Eq. (17d) for convenience.

Following Ref. 1, we define the  $2 \times 2$  matrix  $M_m$  as  $M_m = \prod_{i=1}^{F_m} T_i$ , where  $T_i$  is a matrix  $T_A$  or  $T_B$  in the Fibonacci sequence, and  $X_m = \text{Tr}(M_m)/2$ ; then the bulk-plasmon mode in the Fibonacci HgTe/CdTe superlattice can be written as<sup>1</sup>

$$X_m = \text{Tr}(M_m)/2 = \cos(q_z D_m), \quad (18)$$

where  $D_m$  is the length of the unit cell composed of  $F_m$  elements of the string. Furthermore, if we use the boundary condition for the electric potential at the surface layer, then the surface plasmon mode is given by

$$(\epsilon_s + \epsilon_0 - 2\epsilon_s S_x^{-1}) / (\epsilon_s - \epsilon_0 + 2\epsilon_s S_x^{-1}) + [(M_m)_{11} \pm \exp(-\kappa D_m)] / (M_m)_{12} = 0, \quad (19)$$

where

$$\kappa D_m = \ln[|X_m| + (|X_m|^2 - 1)^{1/2}], \quad (20)$$

and  $S_x^{-1}$  stands for the formal structure factor referred to the different states in the surface layer, i.e.,  $S_E^{-1}$ ,  $S_{\text{LH}}^{-1}$ , or  $S_{\text{HH}}^{-1}$ .

### III. NUMERICAL RESULTS

We now turn to the plasmon spectrum obtained using Eqs. (18) and (19). For the sake of convenience, we only give, as an example, the intrasubband plasmon mode in both the periodic superlattice and the Fibonacci superlattice for comparison. It is evident that the intersubband plasmon mode can be given in a similar way, and it will provide no fundamental difficulty to calculate its spectrum. Moreover, we let  $m=3$  here for simplifying the calculation. The unit cell composed of three elements of the string is shown in Fig. 1(b). Figure 2 presents the intrasubband plasmon spectrum in the periodic HgTe/CdTe superlattice. From it we find that the optical-plasmon mode associated with the heavy-hole-like state is suppressed, due to the Coulomb interaction between the interface states and the bound heavy-hole-like states within the same quantum well. Besides, we also find several attractive surface-plasmon branches which degenerate with two different bulk-plasmon bands in the weak-screening and strong-screening regions, respectively, in comparison with those in type-I and type-II superlattices. In Fig. 3, the intrasubband plasmon spectrum in the Fibonacci HgTe/CdTe superlattice is shown, in which the golden-mean ratio  $d_A/d_B = (\sqrt{5}+1)/2 = 1.618$  is chosen. From it we find that each bulk-plasmon branch is split into three ( $F_3=3$ ) branches in comparison with those in Fig. 2. Here we do not show the surface-plasmon branches, since some of them are too close to

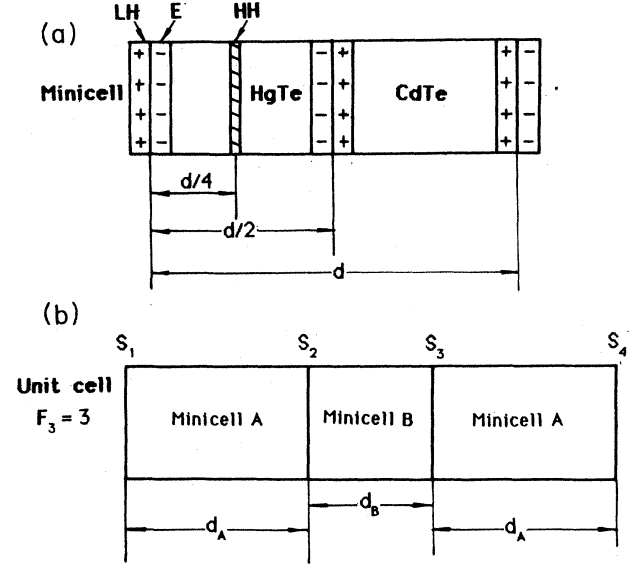


FIG. 1. (a) The minicell of the HgTe/CdTe superlattice. The symbols E, LH, and HH stand for the electron, light-hole, and heavy-hole layers, respectively. (b) The unit cell of the Fibonacci HgTe/CdTe superlattice, in which the Fibonacci number  $F_m$  is chosen as  $F_3=3$ .  $d_A$  and  $d_B$  are the widths of the minicell A and minicell B, respectively.

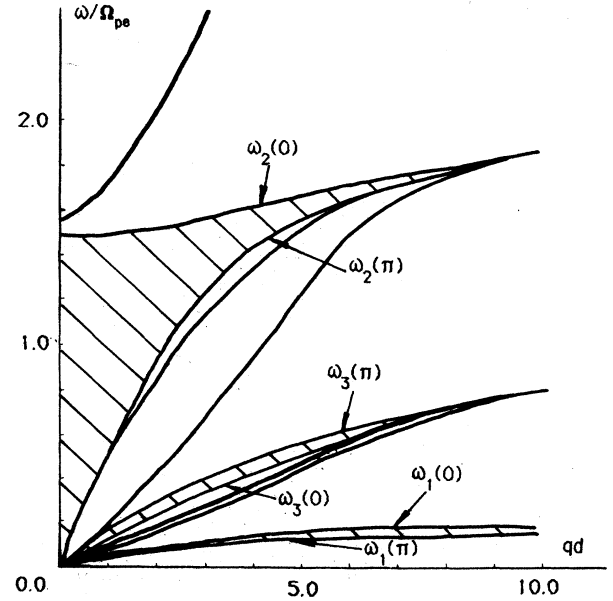


FIG. 2. The plasmon spectrum of the periodic HgTe/CdTe superlattice. The parameters are chosen as  $(\Omega_{\text{hh}}/\Omega_{\text{pe}})^2 = 1/5$ ,  $(\Omega_{\text{ph}}/\Omega_{\text{pe}})^2 = 1/55$ , and  $\beta d = 7.742$ . The symbols  $\Omega_{\text{pe}}$ ,  $\Omega_{\text{ph}}$ , and  $\Omega_{\text{hh}}$  are three-dimensional plasma frequencies of the electron, light hole, and heavy hole, respectively.  $\beta^{-1}$  is the localization length of the interface state.

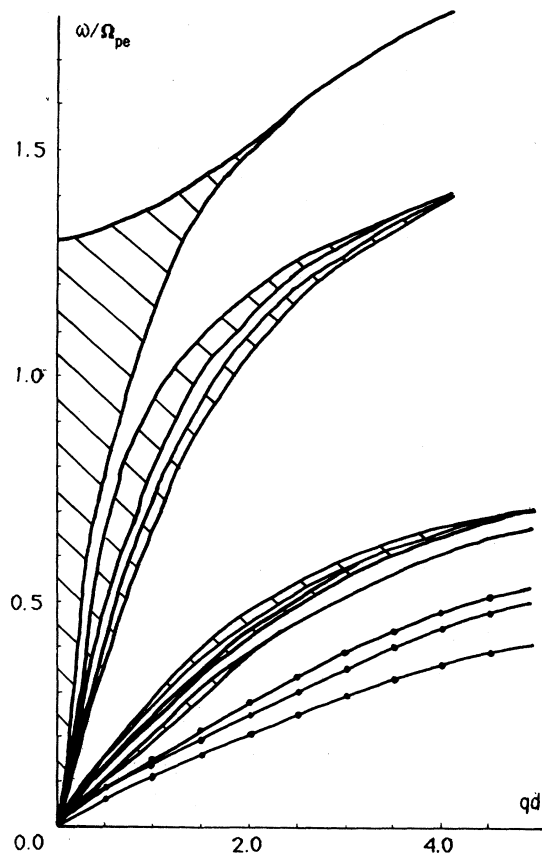


FIG. 3. The plasmon spectrum of the Fibonacci HgTe/CdTe superlattice. The parameters are chosen as  $(\Omega_{hh}/\Omega_{pe})^2 = \frac{1}{5}$ ,  $(\Omega_{ph}/\Omega_{pe})^2 = \frac{1}{10}$ ,  $d_A/d_B = 1.618$ , and  $\beta d_B = 0.7742$ . The symbols  $\Omega_{pe}$ ,  $\Omega_{ph}$ ,  $\Omega_{hh}$ , and  $\beta^{-1}$  have the same meaning as in Fig. 2.

the bulk-plasmon bands to be clearly shown. We should emphasize<sup>1</sup> that as  $m \rightarrow \infty$  we will see an infinite number of very narrow bands which have a typical self-similar Cantor-set structure. From the theoretical analysis, we easily know that there are three different kinds of mini-

cells, corresponding to whether the first charged layer in Fig. 1(a) is selected as an electron, light-hole, or heavy-hole layer, respectively. It leads to the three different features of the bulk-plasmon spectra. On the other hand, there are  $F_m$  different kinds of unit cells composed of  $F_m$  elements of the string for a given minicell, corresponding to whether the first layer is selected at  $S_1, S_2, S_3, S_4, \dots, S_m$ , respectively. This leads to the different features of the surface-plasmon spectra, while the bulk-plasmon spectrum remains the same.

#### IV. DISCUSSION

From the studies above, we know that, in general, there will be three different features of the bulk-plasmon spectra, and for each given bulk-plasmon spectrum, there still exist  $F_m$  different features of the surface-plasmon spectra; thus we will in total get  $3F_m$  different features of the surface-plasmon spectra in such a Fibonacci system.

The electron-phonon coupling can be easily taken into account<sup>6</sup> by replacing the dielectric constant  $\epsilon_s$  with a frequency-dependent one  $\epsilon_s(\omega)$ ,

$$\epsilon_s \longrightarrow \epsilon_s(\omega) = \epsilon_\infty [(\omega^2 - \omega_{LO}^2)/(\omega^2 - \omega_{TO}^2)]. \quad (21)$$

In conclusion, an equivalent-transfer-matrix theory has taken into account the distribution of wave functions within the quantum well, and can also be used to calculate the intersubband plasmon modes in general Fibonacci type-I and type-II superlattices. We expect that this will provide us with useful information about the selection of the surface-plasmon branch in which we are interested for surface-wave device application.

#### ACKNOWLEDGMENTS

This work was supported in part by the Chinese National Science Foundation through Grants No. 1860723 and No. 8688708, and in part by the Chinese Higher Education Foundation through Grant No. 2-1987.

<sup>1</sup>P. Hawrylak, G. Eliasson, and J. J. Quinn, Phys. Rev. B **36**, 6501 (1987).

<sup>2</sup>S. Das Sarma, A. Kobayashi, and R. E. Prange, Phys. Rev. Lett. **56**, 1280 (1986); Phys. Rev. B **34**, 5309 (1986).

<sup>3</sup>P. Hawrylak and J. J. Quinn, Phys. Rev. Lett. **57**, 380 (1986).

<sup>4</sup>R. Merlin, K. Bajema, R. Clarke, F. Y. Juang, and P. K. Bhattacharya, Phys. Rev. Lett. **55**, 1768 (1985); J. Todd, R. Merlin, R. Clarke, K. M. Mohanty, and J. D. Axe, *ibid.* **57**, 1157 (1986).

<sup>5</sup>Dan-hong Huang and Shi-xun Zhou, Phys. Rev. B **38**, 13061 (1988).

<sup>6</sup>Dan-hong Huang and Shi-xun Zhou, Phys. Rev. B **38**, 13069 (1988).

<sup>7</sup>D. Mukherji and B. R. Nag, Phys. Rev. B **12**, 4338 (1975).

<sup>8</sup>Y.-C. Chang, J. N. Schulman, G. Bastard, Y. Guldner, and M. Voos, Phys. Rev. B **31**, 2557 (1985).

<sup>9</sup>M. Jaros, A. Zoryk, and D. Ninno, Phys. Rev. B **35**, 8277 (1987).

<sup>10</sup>Y. R. Lin-Liu, and L. J. Sham, Phys. Rev. B **32**, 5561 (1985).

<sup>11</sup>G. Bastard, Phys. Rev. B **25**, 7584 (1982).

<sup>12</sup>J. M. Berrier, Y. Guldner, and M. Voos, IEEE J. Quantum Electron. **QE-22**, 1793 (1986).

<sup>13</sup>Jean-Pierre Faurie, IEEE J. Quantum Electron. **QE-22**, 1656 (1986).

<sup>14</sup>A. Persson and R. M. Cohen, Phys. Rev. B **38**, 5568 (1988).